41. Our work was funded by the Danish National Research Foundation (Danmarks Grundforskningsfond), a Natural Environment Engineering Research Council Research Fellowship (S.W.P.), the Natural Sciences and Engineering Research Council of Canada, and a Queen's Research Chair. We thank the Parks and Natural Areas, and Government of Newfoundland and Labrador for scientific permits; the Portugal Cove South Interpretation Centre for help and support; and M. Laflamme and L. Salling for help.

Supporting Online Material
www.sciencemag.org/cgi/content/full/1135013/DC1
Materials and Methods
Table S1
References

12 September 2006; accepted 27 October 2006
Published online 7 December 2006;
10.1126/science.1135013
Include this information when citing this paper.

Climate Change Affects Marine Fishes Through the Oxygen Limitation of Thermal Tolerance

Hans O. Pörtner* and Rainer Knust

A cause-and-effect understanding of climate influences on ecosystems requires evaluation of thermal limits of member species and of their ability to cope with changing temperatures. Laboratory data available for marine fish and invertebrates from various climatic regions led to the hypothesis that, as a unifying principle, a mismatch between the demand for oxygen and the capacity of oxygen supply to tissues is the first mechanism to restrict whole-animal tolerance to thermal extremes. We show in the eelpout, *Zoarces viviparus*, a bioindicator fish species for environmental monitoring from North and Baltic Seas (Helcom), that thermally limited oxygen delivery closely matches environmental temperatures beyond which growth performance and abundance decrease. Decrements in aerobic performance in warming seas will thus be the first process to cause extinction or relocation to cooler waters.

Climate change is projected to affect individual organisms, the size and structure of their populations, the species composition of communities, and the structure and functioning of ecosystems. Effects include poleward or high-altitude shifts in the distribution of ectothermic animals (*1*). A comprehensive mechanistic understanding has so far been lacking (*2*) but is needed for prediction of climate change effects. Physiological studies can address the mechanisms and reasons for the thermal sensitivity of organisms and their life stages.

In aquatic animals, a decrease in the capacity to perform aerobically (a drop in aerobic scope) characterizes the onset of thermal limitation at both ends of the thermal envelope [pejus thresholds T_p, fig. S1 (*3*–*6*)]. The reduction in aerobic scope is caused by limited capacity of circulatory and ventilatory systems to match oxygen demand. Such a constraint affects all higher functions (muscular activity, behavior, growth, and reproduction) and might thereby shape the long-term fate of species. Aerobic scope becomes minimal beyond low or high critical temperatures (T_c). Survival is then passive and time-limited, supported by anaerobic metabolism and protection of proteins and membranes by heat shock proteins and antioxidative defense. Thermal tolerance is hierarchical, with narrowing windows from molecular to cellular to systemic levels (*6*). Temperate species are able to acclimatize and shift the thermal window through changes in mitochondrial densities as well as other molecular to systemic adjustments of functional capacities (*3*, *6*–*10*) (fig. S1). Limits to acclimatization are set by trade-offs at various structural and functional levels that constrain the width of the thermal window, for example, through the trend to minimize energy turnover in relation to climate variability (*9*, *10*).

We investigated thermal limitation of the common eelpout, *Zoarces viviparus*, in its southernmost distribution area, the German Wadden Sea (part of the southern North Sea) during summer and thereby tested the ecological relevance of the concept of oxygen- and capacity-limited thermal tolerance (fig. S1). During the past 40 years, water temperatures in the German Bight increased by 1.13°C (at Helgoland Roads). Cold winters with sea surface temperatures (SSTs) around –1°C had occurred about once every 10 years up to 1944 but were experienced only once since 1960 (*11*). Models predict further SST increments for the next 90 to 100 years, by about 1.6° to 3.0°C in the northern and even by 3.0° to 3.9°C in the shallower southern North Sea (*12*), accompanied by rising sea levels (13 to 68 cm by 2050) and an increasing frequency of storm events (*13*).

Comparison of existing data sets indicates that field observations can be explained by the eelpout's physiological responses to warming (Fig. 1). The relative abundance of the nonmigratory eelpout decreases upon warming (5-year running means, data from 1954 to 1989, Fig. 1A) (*14*, *15*), reflecting a higher mortality in hot summers. Reduced field abundance coincides with reduced growth of laboratory-maintained, temperature-acclimated individuals (Fig. 1B). Individual growth is a key parameter shaping population growth and depends on aerobic scope. Lopsided growth curves result from the exponential rise in net aerobic scope upon warming, which is counterbalanced by the concomitant exponential rise in baseline metabolic costs (Fig. 1). Both abundance and growth begin to fall beyond upper pejus temperatures (T_p) (Fig. 1, C to E), reflecting the species-specific limits of acclimation capacity.

Pejus temperatures were derived from limitations in circulatory capacity (Fig. 1C), which occur before ventilatory limitations in eelpout (*Z. viviparus* and *Pachycara brachycephalum*) and Atlantic cod (*Gadus morhua*) (*4*, *16*–*18*). The loss of aerobic scope can also be derived from the shift of critical oxygen tensions, P_c, or concentrations, $[O_2]_c$. P_c or $[O_2]_c$ indicate oxygen limitation to the passive organism in hypoxia and the onset of anaerobic metabolism. Upon warming, $[O_2]_c$ reaches air saturation at T_c, where anaerobic metabolism begins in animals exposed to fully aerated waters (Fig. 1D). Aerobic scope thus begins to fall when $[O_2]_c$ starts to rise beyond T_p (Fig. 1E). Warming exacerbates oxygen limitations not only by the forced rise in oxygen demand, but also by reducing oxygen solubility (Fig. 1E).

The analysis of ecological responses in relation to 5-year running means of summer maxima, albeit improving the signal-to-noise ratio, may not precisely quantify temperatures and mechanisms effective in the field. Analysis of individual summers in long-term data series (*19*) should provide more detailed insight into cause-and-effect relationships (Figs. 2 and 3). The limited data set indicates that extreme temperatures of previous summers cause reduced abundance. Sampling took place in July, so the effects of the hottest season only become visible in the next year. Thermal limitation of aerobic scope may also translate into the next year by reducing the degree of successful fertilization and reproduction.

Thermal sensitivity is likely to be enhanced at large body sizes. In contrast to eelpout from the Baltic or from colder regions like the Russian White Sea, eelpout of the Wadden Sea only reach a maximum body length of about 23 cm at a maximum age of 3 to 4 years (*20*). A preliminary analysis of seasonal changes in size frequency distribution (fig. S2) shows that older specimens (larger than 20 cm) have low overall abundance and thus high mortality rates. High

Alfred Wegener Institute for Polar and Marine Research, Animal Ecophysiology, Postfach 12 01 61, 27515 Bremerhaven, Germany.

*To whom correspondence should be addressed. E-mail: hpoertner@awi-bremerhaven.de

mortality of large fish is probably not associated with predation, which usually occurs during early life stages (*21*). Rather, the oxygen-limitation model predicts that temperature-dependent aerobic limits are experienced earlier by larger than by smaller individuals (*22*). In fact, thermal sensitivity of growth or exercise was found to be enhanced in large compared with small individuals of various fish species (*23*, *24*). Thermal limits depicted in Figs. 1 to 3 are valid for specimens of about 23 cm body length (compare with fig. S2). Mild summers, with temperatures regularly beyond T_p of large fish, can therefore be interpreted to cause mortality of this size class (Fig. 3 and fig. S2). Because of wider thermal windows in smaller specimens, these temperatures still allow for population growth, seen especially during the mild summer of 1998 (Fig. 2). The earlier loss in aerobic scopes of large individuals indicates that specimens do not grow beyond oxygen-dependent size limits set by temperature such that this size group displays low abundance all year round (fig. S2). The species finally experiences a net reduction in abundance (Fig. 1A) when smaller individuals are also affected and population loss during hot summers exceeds yearly population growth. In conclusion, harmful effects of warming set in beyond pejus temperatures. Only summers hotter than critical temperatures of the larger specimens (Figs. 1 to 3) entail the full range of thermal stress phenomena depicted in fig. S1. The mismatch in oxygen supply versus demand thus becomes effective at the ecosystem level before the onset of anaerobic metabolism or of thermal damage (Td in fig. S1) and also before critical thermal maxima (CT_{max}) traditionally determined in thermal biology (*25*).

Overall, the agreement of thermal limits operative in the field with the lab-determined pejus range supports previous studies, which interpreted thermal limitation in aquatic ectotherms to start with limited oxygen supply capacity (*3*–*6*, *16*–*18*) (Fig. 1, C to E). Accordingly, pejus limits are the earliest limits experienced by the whole organism in the field. Decrements in aerobic performance cause reduced growth and enhanced mortality first among larger specimens. A reduction in abundance results when all size groups of a population are affected. Residual variability in the data suggests that not only the temperature value itself but also the length of exposure is crucial in setting mortality. The data did not reveal an influence of the shift to milder winters. Further-

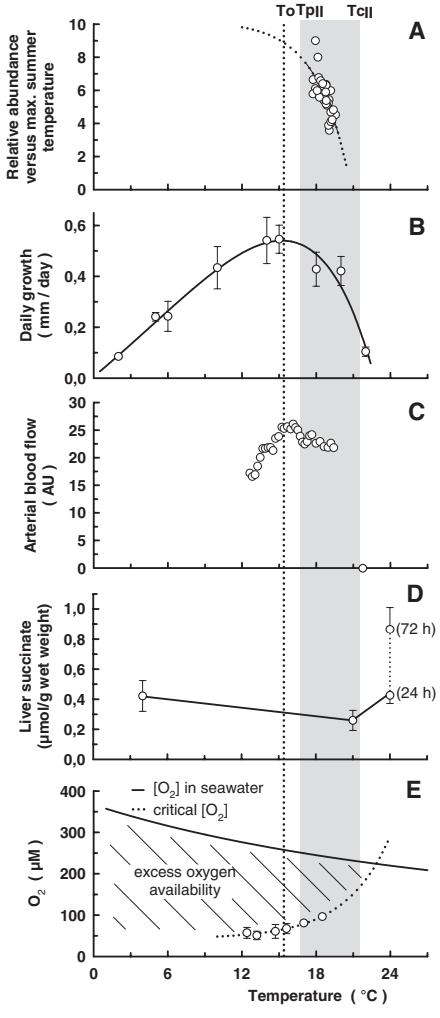

Fig. 1. Matching field and laboratory data reflect thermal limitation in eelpout in accordance with fig. S1. The shaded area characterizes the pejus range between upper T_p and T_c. (**A**) The negative correlation between summer water temperatures and relative abundance indicates heat-induced mortality of eelpout in the Wadden Sea [5-year running mean, recalculated from (*14*, *15*) and weather data licensed by DWD (Deutscher Wetterdienst)]. Data were fitted to $Ar(T) = Ar_{max}[1 - e^{k(T-T_o)}]$ where $Ar(T)$ is the relative abundance depending on temperature ($Ar_{max} = 10.173$; $k = 0.377$; $T_o = 20.853$, $r = 0.7130$, and $P < 0.01$). (**B**) Daily growth increments recalculated from (*31*) in relation to water temperature (mean ± SD). Data were fitted to the equation $dL(T) = F_1(T) + F_2(T) = (A_1 e^{B_1 T} + C_1) + (A_2 e^{B_2 T} + C_2)$ with $dL(T)$ = daily growth rates at maximum food supply. The first term, $F_1(T) = A_1 e^{B_1 T} + C_1$, represents the temperature dependence of aerobic processes supporting growth performance. The second term, $F_2(T) = A_2 e^{B_2 T} + C_2$, represents the parallel, exponential rise in processes limiting aerobic scope and thus growth capacity ($A_1 = 0.9901$, $B_1 = 0.0667$, $C_1 = -0.3953$, $A_2 = -0.1942$, $B_2 = 0.1299$, $C_2 = -0.3953$, $r = 0.9823$, and $P < 0.01$). (**C**) Arterial blood flow in relative units [measured by nuclear magnetic resonance (NMR) imaging techniques and recalculated as running means from (*4*)] reflects maximized circulatory oxygen supply at optimum temperature T_o and capacity limitation beyond T_{pII}. AU, arbitrary units. (**D**) Mismatch between oxygen supply and demand finally leads to the accumulation of succinate in the liver beyond T_{dI} [data are mean ± SD from (*32*)]. (**E**) At upper T_c, $[O_2]_c$ of the eelpout reaches air saturation oxygen concentrations. Water O_2 concentration (solid line) and $[O_2]_c$ (open circles, mean ± SE, fitted by dotted line) were recalculated from (*25*) for a salinity of 32 ‰. $[O_2]_c$ was fitted to $[O_2]_c(T) = C_1 T^{C2} + C_3$ ($C_1 = 4.33 \times 10^{-6}$, $C_2 = 5.56$, $C_3 = 48.19$, $r = 0.9764$, and $P < 0.01$). Reported data are valid for the largest specimens [between 23- and 25-cm body lengths (*25*)] found in the Wadden Sea.

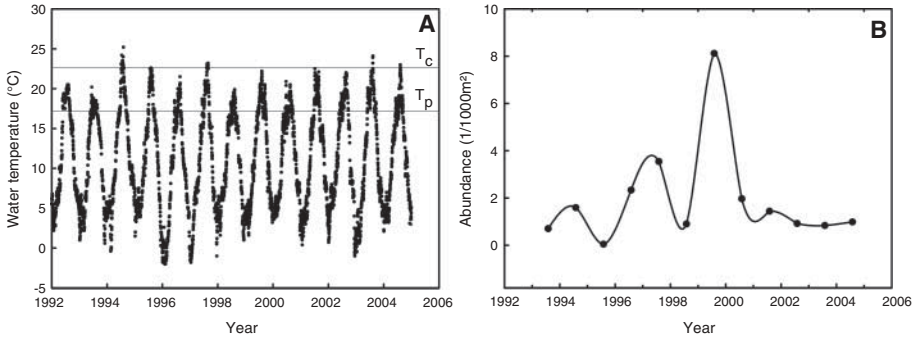

Fig. 2. (**A**) Daily water temperature (°C) in the Wadden Sea from 1992 to 2004 (DWD, Station Norderney). Putative upper critical (T_c) and pejus (T_p) temperatures of large eelpout (Fig. 1) are indicated by horizontal lines. (**B**) Total abundance (1/1000 m^2) of eelpout in the Wadden Sea sampling area during summers between 1993 and 2005. Data fitted by spline curve [Sigmaplot (*33*)].

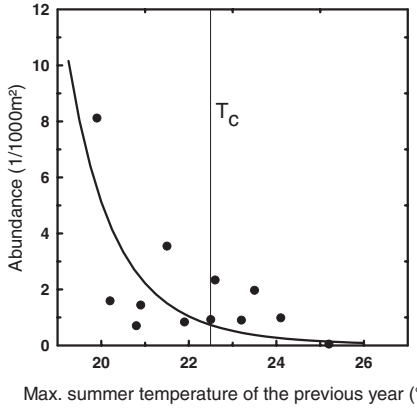

Fig. 3. Abundance of eelpout versus maximum summer temperature from the previous year (data from Fig. 2). Data were fitted to $A(T_{max-1}) = C_1 e^{C_2/C_3 T}$ where $A(T_{max-1})$ is the abundance depending on maximum temperature of the previous summer (fitting parameters $C_1 = 1.2 \times 10^{-7}$, $C_2 = 240.83$, $C_3 = 0.6686$, $r = 0.6599$, and $P < 0.01$). The putative upper T_c (Fig. 1) is indicated by a vertical line.

more, population growth depends on food supply, which in turn influences aerobic performance and thermal sensitivity. Potential additional components in field tolerance still need to be identified. However, we suggest that reduced aerobic performance beyond pejus limits enhances sensitivity to other, more obvious mechanisms eliciting mortality (predation, starvation, or disease). These influences would display their inherent variability and thereby enhance the variability in the temperature-dependence of abundance.

Matching thresholds in field and laboratory data highlight the ecological relevance of the concept of oxygen- and capacity-limited thermal tolerance. Adaptation to climate variability involves adjustments of functional capacity in general and, specifically, in the components of aerobic metabolism, of oxygen supply capacity, and of associated costs. Trade-offs in thermal adaptation processes and in organismic energy budget shape the width of thermal windows, with consequences for biogeography (*1*), growth performance, development, fecundity, recruitment, life-styles, and life-history evolution (*9*, *10*, *26*, *27*). Widths and locations of tolerance windows on the temperature scale may change or shift during ontogeny (*26*). At the ecosystem level, species-specific biogeographical ranges differ but overlap and imply that variable thermal windows and sensitivities cause variability in distribution shifts (*1*), species composition, seasonal timing, and associated mismatch phenomena in species interactions as in a food web. For example, the shift from larger (*Calanus finmarchicus*) to smaller (*C. helgolandicus*) copepod fauna in the southern North Sea caused reduced food availability for Atlantic cod (*G. morhua*) (*28*). This regime shift was largely determined by different thermal windows of the two copepod species (*29*). Warming-induced reductions of cod abundance are thus caused both directly [via thermal sensitivity of cod (*30*)] and indirectly [via the food web (*28*)] but based on the same physiological principles. Overall, the concept of oxygen- and capacity-limited thermal tolerance can provide an integrative framework for developing a cause-and-effect understanding of the influence of climate change and variability on marine ecosystems, including food web structure, recruitment success, and fish landings (*30*).

References and Notes

1. A. L. Perry, P. J. Low, J. R. Ellis, J. D. Reynolds, *Science* **308**, 1912 (2005); published online 12 May 2005 (10.1126/science.1111322).
2. M. N. Jensen, *Science* **299**, 38 (2003).
3. H. O. Pörtner, *Naturwissenschaften* **88**, 137 (2001).
4. F. C. Mark *et al.*, *Am. J. Physiol.* **283**, R1254 (2002).
5. M. Frederich, H. O. Pörtner, *Am. J. Physiol.* **279**, R1531 (2000).
6. H. O. Pörtner, *Comp. Biochem. Physiol.* A **132**, 739 (2002).
7. I. A. Johnston *et al.*, *J. Exp. Biol.* **201**, 1 (1998).
8. I. Hardewig *et al.*, *J. Comp. Physiol. B* **169**, 597 (1999).
9. H. O. Pörtner *et al.*, *Fish Physiol.* **22**, 79 (2005).
10. H. O. Pörtner, *Deep-Sea Res. II* **53**, 1071 (2006).
11. K. H. Wiltshire, B. F. J. Manly, *Helgol. Mar. Res.* **58**, 269 (2004).
12. C. Sheppard, *Mar. Pollut. Bull.* **49**, 12 (2004).
13. Z. W. Kundzewicz, M. L. Parry, in *IPCC: Climate Change 2002: Impacts, Adaptation, and Vulnerability*, J. J. McCarthy *et al.*, Eds. (Cambridge Univ. Press, Cambridge, 2001), pp. 641–692.
14. K. Tiews, *Arch. Fischereiwiss.* **34**, 4 (1983).
15. K. Tiews, H. Wienberg, *Veröff. Inst. Küsten Binnenfisch. Hamburg* **103**, 1 (1990).
16. H. O. Pörtner *et al.*, *Respir. Physiol. Neurobiol.* **141**, 243 (2004).
17. G. Lannig *et al.*, *Am. J. Physiol.* **287**, R902 (2004).
18. F. J. Sartoris *et al.*, *J. Fish Biol.* **62**, 1239 (2003).
19. Materials and methods are available on *Science* Online.
20. J. Ulleweit, thesis, University at Bremen, Bremen, Germany (1995).
21. S. M. Sogard, *Bull. Mar. Sci.* **60**, 1129 (1997).
22. H. O. Pörtner, *Physiol. Biochem. Zool.* **77**, 959 (2004).
23. T. K. Linton *et al.*, *Can. J. Fish. Aquat. Sci.* **55**, 576 (1998).
24. K. J. Rodnick *et al.*, *J. Fish Biol.* **64**, 310 (2004).
25. M. V. Zakhartsev *et al.*, *J. Comp. Physiol. B* **173**, 365 (2003).
26. H. O. Pörtner *et al.*, *Physiol. Biochem. Zool.* **79**, 295 (2006).
27. H. O. Pörtner, *J. Exp. Biol.* **205**, 2217 (2002).
28. G. Beaugrand *et al.*, *Nature* **426**, 661 (2003).
29. P. Helaouët, G. Beaugrand, *Mar. Ecol. Progr. Ser.*, in press.
30. H. O. Pörtner *et al.*, *Cont. Shelf Res.* **21**, 1975 (2001).
31. M. Fonds *et al.*, (Demersal Fish Committee), *Metabolism, Food Consumption, Growth, and Food Conversion of Shorthorn Sculpin* (Myoxocephalus scorpius) *and Eelpout* (Zoarces viviparus) (Document G:31, International Council for Exploration of the Sea, Copenhagen, 1989).
32. P. L. M. van Dijk *et al.*, *J. Exp. Biol.* **202**, 3611 (1999).
33. Sigmaplot, Systat Software Incorporated, San Jose, CA.

34. Supported by the MarCoPoll program of the Alfred Wegener Institute.

Supporting Online Material

www.sciencemag.org/cgi/content/full/315/5808/95/DC1
Materials and Methods
Figs. S1 and S2

22 September 2006; accepted 29 November 2006
10.1126/science.1135471

A Hexanucleotide Element Directs MicroRNA Nuclear Import

Hun-Way Hwang,[1] Erik A. Wentzel,[2] Joshua T. Mendell[1,2]*

MicroRNAs (miRNAs) negatively regulate partially complementary target messenger RNAs. Target selection in animals is dictated primarily by sequences at the miRNA 5′ end. We demonstrated that despite their small size, specific miRNAs contain additional sequence elements that control their posttranscriptional behavior, including their subcellular localization. We showed that human miR-29b, in contrast to other studied animal miRNAs, is predominantly localized to the nucleus. The distinctive hexanucleotide terminal motif of miR-29b acts as a transferable nuclear localization element that directs nuclear enrichment of miRNAs or small interfering RNAs to which it is attached. Our results indicate that miRNAs sharing common 5′ sequences, considered to be largely redundant, might have distinct functions because of the influence of cis-acting regulatory motifs.

Nucleotides 2 to 7 of microRNAs (miRNAs), known as "seed" sequences, are considered the most critical for selecting targets. Within a given species, highly related miRNAs sharing a common seed sequence are grouped into miRNA families, are predicted to have overlapping targets, and are considered to be largely redundant (*1*–*5*). Nevertheless, loss of function of miRNA family members with divergent 3′ end sequences results in overlapping but distinct phenotypes in *Caenorhabditis elegans* and in *Drosophila* (*6*, *7*). These distinct phenotypes often do not appear to be due to differences in miRNA expression patterns, which raises the possibility that distinct sequences within miRNA family members confer upon them characteristic functional properties. Here we describe a sequence motif that dramatically influences the posttranscriptional behavior of a human miRNA.

Examination of cell-cycle stage–specific miRNA expression patterns with a previously described oligonucleotide array (*8*) revealed substantial accumulation of miR-29 in mitotic HeLa cells (*9*). There are three human miR-29 paralogs: miR-29a, miR-29b, and miR-29c (fig. S1A). A highly specific Northern blot assay (fig. S1B) demonstrated that each exhibits a distinct expression pattern. miR-29a is constitutively expressed in all cell-cycle phases, miR-29b is present at low levels except in mitotic cells, and miR-29c is not detectable (Fig. 1A).

Human miR-29 family members are encoded by the miR-29b-1/miR-29a cluster and the miR-29b-2/miR-29c cluster (Fig. 1B). A fragment encompassing the miR-29b-1/miR-29a cluster was amplified by reverse transcription polymerase chain reaction (RT-PCR) after small interfering RNA (siRNA)–mediated inhibition of Drosha (which performs the first step in

[1]Program in Human Genetics and Molecular Biology, McKusick-Nathans Institute of Genetic Medicine, Johns Hopkins University School of Medicine, Baltimore, MD 21205, USA. [2]McKusick-Nathans Institute of Genetic Medicine, Johns Hopkins University School of Medicine, Baltimore, MD 21205, USA.

*To whom correspondence should be addressed. E-mail: jmendell@jhmi.edu